Use of Modern Electron Transfer Theories To Determine Electronic Coupling Matrix Elements in Intramolecular Systems

Krishna Kumar,[†] Igor V. Kurnikov,[‡] David N. Beratan,[‡] David H. Waldeck,*[,‡] and Matthew B. Zimmt*[,†]

Department of Chemistry, Brown University, Providence, Rhode Island 02912, and Department of Chemistry, University of Pittsburgh, Pittsburgh, Pennsylvania 15260

Received: November 6, 1997; In Final Form: March 2, 1998

The dependence of the donor/acceptor electronic coupling on the topology of donor−bridge−acceptor (DBA) molecules is probed experimentally and theoretically. The temperature dependence of photoinduced electron-transfer rate constants is analyzed with a semiclassical electron-transfer model to extract the donor/acceptor electronic coupling matrix elements $|V|$ and the low-frequency reorganization energy at 295 K, λ_o(295 K), for four rigid DBA molecules. The sensitivity of the electronic coupling $|V|$ to the models and parameters used to fit the data are extensively investigated. The treatment of the low-frequency reorganization energy's temperature dependence has a significant impact on the analysis. The identity of the principal coupling pathways is determined for molecular linkages that propagate symmetry allowed donor/acceptor interactions and molecular linkages that propagate symmetry forbidden donor/acceptor interactions. For the symmetry forbidden case, these analyses demonstrate that solvent molecules provide the dominant coupling pathway in the nine-bond bridge, C-shaped molecule **2** but do not significantly influence $|V|$ across the seven-bond, linear bridge in **1**.

1. Introduction

An interesting challenge in the study of electron-transfer reactions is to identify and probe structural elements that promote electronic coupling ($|V|$) between an electron donor (D) and an electron acceptor (A). In systems where the strength of the electronic coupling between the donor and the acceptor (in frequency units) is smaller than the reciprocal time spent in the transition state region, the associated electron-transfer reactions are classified as nonadiabatic.[1,2] In this regime, the Golden Rule predicts that the electron-transfer rate constant, k_{ET}, is proportional to the square of the donor/acceptor electronic coupling, namely,

$$k_{ET} = \frac{2\pi}{\hbar}|V|^2\mathrm{FCWDS} \qquad (1)$$

where FCWDS is the Franck−Condon weighted density of states.[3] As a result, electron-transfer rate constant measurements in nonadiabatic systems provide a means to explore the dependence of donor/acceptor electronic coupling on molecular properties and structure.

The Golden Rule rate expression (eq 1) depends on nuclear geometries, mainly through the Franck−Condon term. Theoretical[2−4] and experimental[5] studies demonstrate the many orders of magnitude impact that the FCWDS exerts on the rate constant. To obtain meaningful estimates of $|V|$ from rate data, the FCWDS must be determined accurately. For large organic systems, accurate evaluation of the FCWDS is very difficult. Instead, numerous groups[5] have successfully employed a single quantized mode, semiclassical expression[3b] (eq 2) to interpret electron-transfer rate constant data in a wide variety of donor/acceptor systems. Within this formulation, the semiclassical electron-transfer rate constant k_{ET} is controlled by five parameters: $|V|$, the donor/acceptor electronic coupling matrix element; $-\Delta G°$, the reaction driving force; λ_o, the low-frequency (primarily solvent) reorganization energy; λ_V, the high-frequency reorganization energy arising from structural changes of the donor and acceptor upon electron transfer; and $\hbar\omega$, the average energy spacing of the effective quantized mode undergoing reorganization upon electron transfer.

$$k_{ET} = \frac{2\pi|V|^2}{\hbar[4\pi kT\lambda_o]^{1/2}}\sum_{n=0}^{\infty} e^{-S}\left(\frac{S^n}{n!}\right)\exp\left[\frac{-(\Delta G° + \lambda_o + n\hbar\omega)^2}{4\lambda_o kT}\right]; \quad S = \lambda_V/\hbar\omega \qquad (2)$$

Different approaches have been used to evaluate the four quantities in the FCWDS expression and $|V|$. Plots of electron-transfer rate constants versus driving force, through the Marcus normal[5f] and inverted[5b,c] regions, provide impressive demonstrations of the utility of eq 2 and yield useful estimates of $|V|$, λ_o and λ_V. Simultaneous analyses of charge-transfer absorption and emission spectra[5c,6] yield accurate determinations of $\Delta G°$ and estimates of λ_o, $\hbar\omega$, and λ_V. Resonance Raman[7] studies of ground-state charge-transfer complexes characterize structural changes attending electron transfer and allow for more elaborate parametrization of semiclassical models of the FCWDS. The temperature dependence of electron-transfer rate constants has also been employed to evaluate FCWDS and to characterize the reorganization parameters.[8−10] The latter approach is used in this study.

This paper uses the semiclassical model (eq 2) and temperature-dependent rate data to extract values for the electronic coupling $|V|$ and compares these values to those computed using

* To whom correspondence should be addressed.
[†] Brown University.
[‡] University of Pittsburgh.

S1089-5639(98)00113-3 CCC: $15.00
Published on Web 04/22/1998

CHART 1

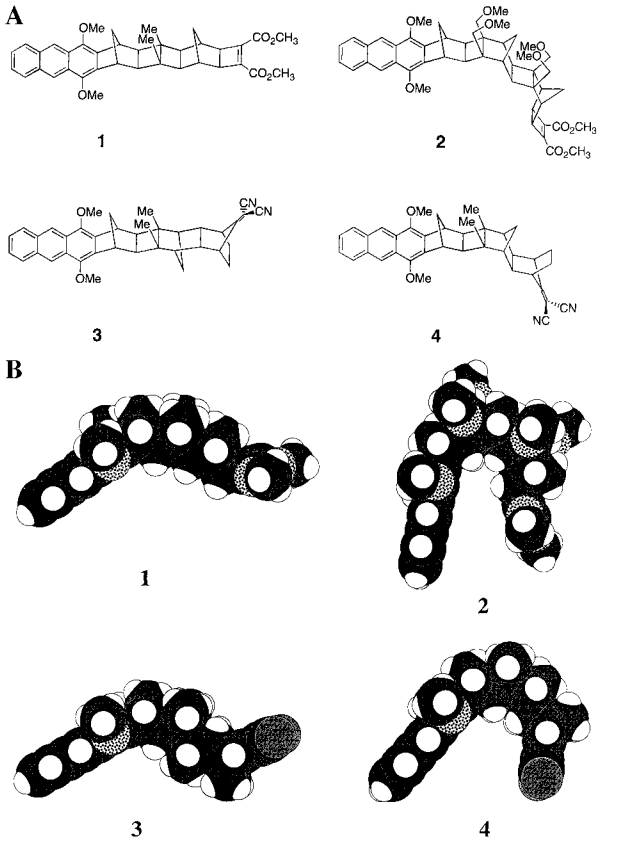

ab initio and semiempirical methods. The aim of the analysis is to determine the relative importance of through bond and through solvent coupling pathways. The donor−bridge−acceptor/solvent systems analyzed here (Chart 1) are taken from prior experimental investigations of symmetry effects[9] and solvent mediation[10] of donor/acceptor coupling. Because of the large number of parameters in the electron-transfer rate model (eq 2), a detailed inquiry into the dependence of $|V|$ on the modeling is presented. The parameters used to simulate the FCWDS cause significant changes in the value of $|V|$ that is obtained from the data. By exploring the sensitivity of $|V|$ to the parameters and the modeling, it is possible to characterize the uncertainty in the value of $|V|$ one obtains from the rate data.

Three aspects of the kinetic models used to calculate the rate constants are investigated. First, both the electron-transfer driving force and the low-frequency (solvent) reorganization energy vary with temperature.[8a,b,11] To analyze the rate data as a function of temperature, specific models of $\Delta G°(T)$ and $\lambda_o(T)$ must be assumed. In this paper, the temperature dependencies of these quantities are modeled using (i) conventional continuum models,[8b,11c] (ii) recently developed continuum algorithms (FDPB[12]) that explicitly account for the molecular shape and charge distributions of the ionic and neutral DBA,[13,43b] or (iii) molecular models of solvation proposed by Matyushov.[14] Second, despite information obtained from analysis of charge-transfer emission spectra and structural calculations, the most appropriate values of $\hbar\omega$ and λ_V, within the single quantized mode approximation, are not known. Thus, this paper explores the correlations between extracted values of $|V|$ and the values assumed for λ_V as well as for $\Delta G°(295\ K)$. Third, eq 2 incorporates one of numerous possible approximate descriptions of the FCWDS. Two quantized mode and classical (no quantized modes) approximations are often used to analyze electron-transfer data. This paper also explores the dependence of $|V|$ on the number of quantized modes employed in the calculation of the FCWDS.

These inquiries provide insight into the origin and magnitude of uncertainty in $|V|$ values that are extracted from temperature dependence data. It appears that uncertainty in λ_V (values ranging from 0.0 to 0.5 eV) translates into less than a factor of 3 uncertainty in the magnitude of $|V|$. Use of different models for $\Delta G°(T)$ and $\lambda_o(T)$ can also generate significant variations in $|V|$. The modeling of the these two parameters is explored extensively. Importantly, in comparisons among DBA/solvent systems with the same donor and acceptor but different bridge structures, the variations of $|V|$ resulting from different models and parameters are such that the relative magnitudes of $|V|$ remain nearly constant. This result allows robust conclusions to be drawn concerning solvent mediated superexchange. Finally, comparisons of DBA molecules with different donor and acceptor orientations relative to the bridge demonstrate that $|V|$ in symmetry allowed DBA molecules is at least 1 order of magnitude larger than for symmetry forbidden DBA molecules with comparable length bridges.

The remainder of this paper is divided into eight sections. In the next section (II) the modeling of the parameters in the semiclassical expression is described. In section III, the one quantum mode model is used to simulate the rate constants for **1** and **2**, and values of $|V|$ and $\lambda_o(295\ K)$ are extracted from the data. Section IV addresses the impact of zero and two quantized mode models on the values of $|V|$ for **1** and **2**. Section V of the paper describes the electronic coupling in **3** and **4** and investigates the possible role of solvent mediated superexchange for the symmetry allowed systems. Section VI compares the electronic couplings obtained from the data with theoretically predicted values. Section VII discusses the results of the analyses, and section VIII draws conclusions about the electronic coupling values and the importance of solvent mediated electronic coupling.

II. Overview of Models and Parameters Used To Analyze the Electron-Transfer Rate Constants

Temperature-dependent electron-transfer rate constants are commonly interpreted using a single quantized mode, semiclassical rate expression (eq 2). Such an analysis requires five "fundamental parameters" (λ_o, λ_V, $\hbar\omega$, $|V|$, and $\Delta G°$) and their individual temperature dependencies. It is usually assumed that $|V|$, λ_V, and $\hbar\omega$ are temperature independent. The latter two quantities arise from high-frequency quantized modes coupled to the electron-transfer event. The initial populations, the frequencies, and the displacements of these modes are unlikely to change over the temperature range employed in these investigations. Thus, the assumed temperature independence of these quantities appears reasonable.[11b] In the absence of prompting experimental results, $|V|$ is also assumed to be temperature independent. The challenge is to constrain the values of the other four parameters (λ_o, λ_V, $\hbar\omega$, and $\Delta G°$) and the temperature dependencies of λ_o and $\Delta G°$. Because the temperature dependence of the rate constant is well-described by an Arrhenius type of analysis (see Figure 1), only two parameters can be extracted from the data. The approach taken here is to extract λ_o at 295 K and $|V|$ from the temperature-dependent kinetic data and to model the other parameters and temperature dependencies.

A. Modeling the Quantized Mode (λ_V and $\hbar\omega$). Appropriate values for λ_V and $\hbar\omega$ were estimated in two ways. First, the charge-transfer emission band shapes[5c,15] from shorter (three-

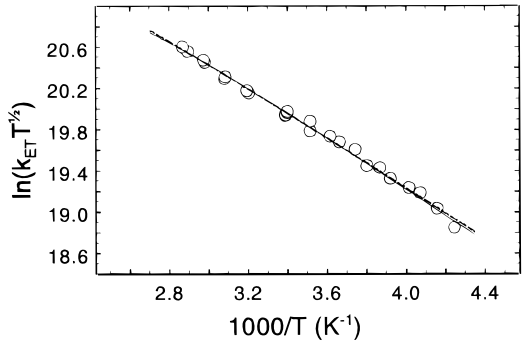

Figure 1. Experimental k_{ET} data (circles) for **1** in acetonitrile with regression fits obtained using $\lambda_V = 0.39$ eV and $\Delta G°(295\ \text{K}) = -0.1$, -0.55, or -0.8 eV.

TABLE 1: Comparison of Theoretical and Experimental Values for the Internal Reorganization Energy λ_V (eV)

method	1 and 2	3 and 4	TCNE[18]
HF 3-21G (CIS)	0.70	0.52	0.26
MP2/6-31G(d)	0.46	0.42	0.35
AM1	0.53	0.31	
exp	0.30−0.50	0.30−0.50	0.13−0.26

and four-bond bridge) analogues[16] of **1**−**4** were analyzed to obtain λ_V and $\hbar\omega$. Second, ab initio calculations of the geometry changes in the donor and acceptor upon charge-transfer were used to calculate λ_V and $\hbar\omega$.

In principle, values of $\Delta G°$, λ_o, λ_V, and $\hbar\omega$ can be obtained by analyzing charge-transfer spectra. However, different values of the four parameters generate equally acceptable fits of the charge-transfer spectra and, thus, do not sufficiently constrain their values.[17] For this reason semiempirical calculations (AM1 level) of the donor and acceptor geometries before and after charge transfer were used to guide the analysis and to identify reasonable parameter ranges (see Table 1).[9b] Acceptable values of λ_V ranging from 0.3 to 0.5 eV and values of $\hbar\omega$ ranging from 1100 to 1800 cm^{-1} were obtained from a compound having the same donor and acceptor groups as **1** and **2**. A similar range of values was found for **3** and **4**. In the latter case, the values of λ_V and $\hbar\omega$ are consistent with those found for charge-transfer complexes involving tetracyanoethylene (TCNE).[18]

In an effort to obtain better theoretical estimates of λ_V and $\hbar\omega$, ab initio calculations of the geometry changes for the donor and acceptor moieties upon charge-transfer were performed. Configuration interaction singles (CIS) for the excited state and Hartree−Fock with a 3-21G basis set for the cation state were used to describe the donor group (dimethoxyanthracene). Hartree−Fock and MP2 calculations using 3-21G, 6-31G, and 6-31+G(d) basis sets were employed to describe the anion and neutral forms of the acceptor. The values for the internal reorganization energy are compiled in Table 1. The calculations indicate that the internal reorganization energy is dominated by the acceptor. The donor anthracene moiety contributes 0.12 eV to the total inner sphere reorganization energy. The acceptor in **1** and **2** contributes from 0.34 to 0.58 eV, and the acceptor in **3** and **4** contributes from 0.30 to 0.40 eV. For these systems, the geometry changes are mainly attributable to displacements in the carbon−carbon bond lengths, which is consistent with frequencies in the 1400 ± 200 cm^{-1} region being coupled to the electron transfer. This range of values for the inner sphere reorganization energy and frequencies is consistent with those obtained from fits to the charge-transfer spectra.

These analyses were used to choose a physically reasonable range of values for $\hbar\omega$ and λ_V. In the absence of specific information, $\hbar\omega$ was fixed at 0.175 eV (1412 cm^{-1}) for all of the DBA systems. A variation in $\hbar\omega$ of ±200 cm^{-1} (at constant S)[19] has little effect on the calculated rate constant. This insensitivity to the value of $\hbar\omega$ occurs because the summand in eq 2 with $n = 0$ (independent of $\hbar\omega$) is the dominant contributor to the rate expression. Of greater concern is the broad range of values for the λ_V of DBAs **1**−**4**.[16] An inappropriate value of the reorganization energy can significantly alter the extracted values of $|V|$. To explore this sensitivity, the electron-transfer data were analyzed using values of λ_V ranging from 0 to 0.5 eV.[20] This range of vibrational reorganization energies encompasses the values that are commonly found for organic DBA molecules and is consistent with the estimates made here. The electronic couplings and reorganization energies reported in Tables 2−4 assume particular values of λ_V. For **1** and **2**, λ_V was chosen to be 0.39 eV, and for **3** and **4**, it was chosen to be 0.30 eV. The lower value of λ_V for **3** and **4** was chosen to reflect the consistently lower values obtained for it in the computations (see Table 1).

B. Modeling the Reaction Free Energy and Its Temperature Dependence. The reaction free energy $\Delta G°$ plays a key role in determining the electron-transfer rate. It is important to explore the sensitivity of the best fit value of $|V|$ and $\lambda_o(295\ \text{K})$ to $\Delta G°$ and the assumed form of its temperature dependence. Rehm and Weller[21] estimated the formation free energy of a solvent separated ion pair from an excited precursor pair as

$$\Delta G° = -E_{00} + E_{\text{OX}} - E_{\text{RED}} + C \tag{3}$$

where E_{00} is the zero−zero transition energy for optical excitation, E_{OX} is the oxidation potential of the ground-state donor, and E_{RED} is the reduction potential of the ground-state acceptor. To a first approximation, C is the Coulomb energy change resulting from electron transfer between the donor and acceptor species in solution. Two models based on eq 3 were employed to estimate $\Delta G°$ in different solvents and at different temperatures. Both models used the same E_{00} value for the donor and the same redox potentials for the donor and acceptor in acetonitrile. The models differ in the manner in which the Coulomb attraction and ion solvation are evaluated.

The first model assumes that the ions are spherical, and the Born equation is used to compute the electrostatic solvation energy. The reaction free energy $\Delta G°(T)$ is given by

$$\Delta G°(T) = -E_{00} + E_{\text{OX}} - E_{\text{RED}} + \frac{e^2}{2}\left(\frac{1}{r_A} + \frac{1}{r_D} - \frac{2}{R_{CC}}\right)\left(\frac{1}{\epsilon(T)} - \frac{1}{\epsilon_{\text{REF}}}\right) - \frac{e^2}{\epsilon_{\text{REF}} R_{CC}} \tag{4}$$

where r_A and r_D are effective radii of the reduced acceptor and oxidized donor ions, R_{CC} is the center to center distance between the ions, $\epsilon(T)$ is the dielectric constant of the solvent in which the electron-transfer reaction occurs, and ϵ_{REF} is the static dielectric constant of the solvent used to measure E_{OX} and E_{RED}. The last term in eq 4 is the Coulomb stabilization of the oppositely charged product ions, and the second to last term arises from the separation-distance-dependent solvation energy of the ion pair. In this model, the reaction free energy's temperature dependence arises from the temperature-dependent dielectric constant.

Although eq 4 provides a convenient means for estimating $\Delta G°(T)$, the absolute accuracy of the calculated values is questionable. This inaccuracy arises from the choice of parameters in the model, as well as from the underlying assumptions. For example, the ionic radii and separation distance for nonspherical reactants are ill-defined. Also, to the

TABLE 2: Comparison of Computed Solvent Reorganization Energies λ_o(295 K) and Those Obtained from Rate Data (eV)[a]

system	Marcus	FDPB[b]	method 1[c]	method 2[c]	method 3[c]	$\Delta G°$(295 K)[c]
1/CH_3CN	1.03	1.05−1.19	1.49 ±0.08	1.19 ± 0.08	1.01 ± 0.07	−0.54
1/PhCN	0.76	0.80−0.89	1.16 ± 0.08	0.94 ± 0.09	0.78 ± 0.06	−0.50
1/DMA	0.89	0.93−1.03	1.30 ± 0.08	1.03 ± 0.09	0.84 ± 0.04	−0.54
1/THF[d]	0.73	0.72−0.80	1.18 ± 0.06	0.80 ± 0.08		−0.38
2/CH_3CN	0.62	0.80−0.90	1.24 ± 0.07	1.07 ± 0.08	0.79 ± 0.05	−0.56
2/CH_3CN[e]		0.73−0.83	1.24 ± 0.09			
2/PhCN	0.46	0.61−0.70	1.12 ± 0.10	0.99 ± 0.10	0.85 ± 0.07	−0.53
2/PhCN[e]		0.53−0.62				
2/DMA	0.54	0.70−0.78	0.95 ± 0.06	0.74 ± 0.10	0.60 ± 0.06	−0.56
3/CH_3CN	1.05	1.16−1.27	1.62 ± 0.08	1.34 ± 0.10	1.17 ± 0.07	−0.26
3/PhCN	0.78	0.87−0.97	1.27 ± 0.09	1.02 ± 0.09	0.90 ± 0.07	−0.21
3/THF[d]	0.73	0.78−0.88	1.28 ± 0.07	0.74 ± 0.09		−0.10
4/CH_3CN	0.78	0.91−1.05	1.54 ± 0.09	1.33 ± 0.09	1.03 ± 0.06	−0.28
4/THF[d]	0.56	0.62−0.72	1.05 ± 0.07	0.69 ± 0.09		−0.16

[a] CH_3CN is acetonitrile; PhCN is benzonitrile; DMA is dimethylacetamide; THF is tetrahydrofuran. [b] The range of values found using the FDPB method correspond to different atomic radii as input parameters. The extremes shown represent 2.1 and 2.3 Å for a carbon atom. [c] The uncertainty in the λ_o values represents their variation with $\Delta G°$(295 K) and λ_V. The range of $\Delta G°$(295 K) values was taken to be ±0.05 eV of the value in the last column. For **1** and **2**, $0.3 < \lambda_V < 0.5$ eV. For **3** and **4**, 0.20 eV $< \lambda_V <$ 0.40 eV. Method 1: $\Delta G°(T) - \Delta G°$(295 K) calculated with eq 4; $\Delta\lambda_o(T)$ calculated with eq 6. Method 2: $\Delta G°$ and λ_o treated as temperature independent. Method 3: $\Delta G°(T) - \Delta G°$(295 K) calculated with eq 4; $\Delta\lambda_o(T)$ calculated with eq 9 and as described in the text. [d] Matyushov's theory for λ_o should not be used with weakly polar solvents.[14] [e] These FDPB calculations were performed with the solvent excluded from the cleft.

TABLE 3: Values of $|V|$ (cm^{-1}) That Are Obtained from Temperature-Dependent Rate Data[a]

systems	method 1[b]	method 2[b]	method 3[b]	ΔG° (eV)[c]
1/CH_3CN	19 ± 4	5.2 ± 1.2	2.5 ± 0.7	−0.54
1/PhCN	15 ± 4	4.6 ± 1.0	2.9 ± 0.8	−0.50
1/DMA	18 ± 4	5.3 ± 1.1	2.4 ± 0.7	−0.54
1/THF	20 ± 7	3.5 ± 0.9		−0.38
2/CH_3CN	24 ± 5	11.5 ± 2.4	4.1± 1.0	−0.56
2/PhCN	73 ± 15	40 ± 10	22 ± 5	−0.53
2/DMA	17 ± 3	8.0 ± 1.1	5.3 ± 0.9	−0.56
3/CH_3CN	375 ±100	98 ± 26	40 ± 12	−0.26
3/PhCN	260 ± 75	74 ± 17	41 ± 13	−0.21
3/THF	600 ± 250	37 ± 11		−0.10
4/CH_3CN	240 ± 70	87 ± 23	20 ± 7	−0.28
4/THF	135 ± 50	23 ± 6		−0.16

[a] CH_3CN is acetonitrile; PhCN is benzonitrile; DMA is dimethylacetamide; THF is tetrahydrofuran. [b] For a description of the methods, see footnote *c* to Table 2. [c] This is the driving force estimate obtained from eq 4. The uncertainty in the $|V|$ values represents their variation with $\Delta G°$(295 K) and λ_V. For the range of $\Delta G°$ and λ_V values see footnote *c* to Table 2.

TABLE 4: Comparison of Experimental and Theoretical Couplings (in cm^{-1}) for the DBA Molecules in Acetonitrile and Benzonitrile

theoretical results			experimental results		
species	ab initio	generalized MH	species	method 2	method 3
1/in vacuo	5.5	4.1			
			1/ACN	5.2	2.5
			1/PhCN	4.6	2.9
2/in vacuo	0.02	0.08			
2/ACN[a]	81	7.1	**2**/ACN	12	4
2/PhCN[a]	62	46	**2**/PhCN	40	22
3/in vacuo	71	75			
			3/ACN	98	41
4/in vacuo	121	12			
4/ACN[a]	145		**4**/ACN	87	20

[a] This species had a solvent molecule located between the donor and acceptor moieties.[42]

extent that the dielectric constant is meaningful on the length scale of a single molecule, the choice of a value for the dielectric constant is not clear when the donor and acceptor are connected by an extended bridge whose polarity and polarizability differ from those of the solvent. Another difficulty lies in the oversimplified treatment of the interactions between the ion reaction fields. At distances where the cation−anion interaction is large, the reaction fields of the ions overlap and reduce the solvation of the ions, as compared to two separated ions.[22] For systems with the donor and acceptor in close proximity, eq 4 overestimates the driving force of charge separation. This source of error in the simple continuum model is expected to be important for **2** which has a donor to acceptor separation of about 7 Å.

The second model for $\Delta G°$ uses a finite difference solution of the Poisson−Boltzmann equation (FDPB[12]) to evaluate the Coulomb and solvation terms.[23] $\Delta G°$ was calculated using these quantities and the thermodynamic cycle in the Appendix. This model accounts explicitly for the molecular shape and extended charge distribution change upon electron transfer in the DBA molecules, on the basis of electronic structure calculations. The solvent is modeled as a continuum with a frequency-independent dielectric constant. The solute is represented by a set of point charges placed into a cavity of lower dielectric constant (chosen to be $\epsilon_{IN} = 2.0$ in order to mimic the electronic polarizability of the solute). The charges on each atomic site were obtained from ab initio calculations using CIS and the Hartree−Fock method with a 3-21G basis set and the Merz−Kollman charge fitting scheme.[24] The boundary between the solute and solvent was generated by rolling a probe solvent molecule (approximated by a sphere of 2.5 Å radius) along the van der Waals surface of the solute. All points inaccessible to the probe sphere's surface are considered to belong to the solute. The dielectric constant in the outer region is that for the solvent of interest.

The most important parameters that enter the FDPB calculation are the radii of the solute atoms and the effective radius of the probe solvent molecule. Atomic radii define the size of the solute cavity or how close the solvent charges may come to the solute. Thus, solute effective atomic radii depend on properties of the *solvent*. For a solute with a complicated shape (e.g., **2**) the extent of the cavity and the results of the FDPB calculation are significantly influenced by the solvent radius parameter. In the experiments analyzed here, the solvents were acetonitrile, benzonitrile, dimethylacetamide, and tetrahydrofuran (THF). The atomic radius parameters in these calculations were optimized for acetonitrile using experimental redox potentials, ionization potentials, and electron affinities of

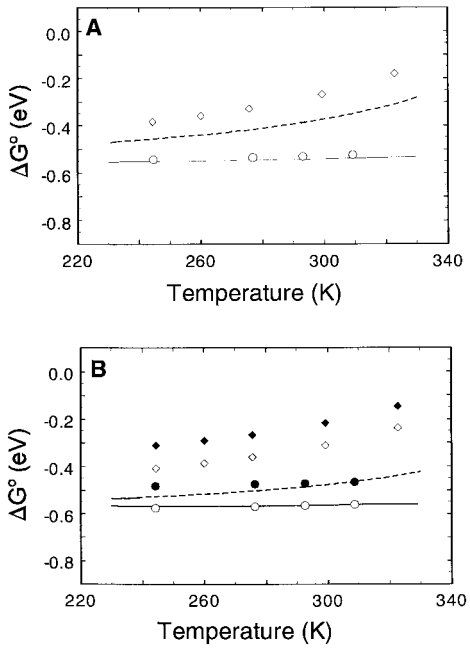

Figure 2. Comparison of the calculated $\Delta G°(T)$ using eq 4 and the FDPB method. For eq 4 (solid line is acetonitrile and dashed line is THF), $r_X^{-1} = 4.5$ Å, R_{CC}=11.5 Å for **1** (panel A) and $R_{CC} = 7.1$ Å for **2** (panel B). The filled symbols are the results of FDPB calculations in which the dielectric is excluded from the cleft between the donor and acceptor ($\epsilon_{IN} = 2$) and the open symbols are the results of FDPB calculations in which the dielectric fills the cleft. Panel A: **1** in THF (◇) and acetonitrile (○). Panel B: **2** in THF (◇ and ◆) and in acetonitrile (○ and ●).

aromatic hydrocarbons. Details of this calibration procedure are provided in the Supporting Information.

Both of these models for $\Delta G°$ treat the solvent as a dielectric continuum but differ as to the degree of realism in treating the molecular shape and molecular charge distribution. The first model provides a point of reference with previous work. The calculated $\Delta G°(T)$ values for **1** and **2** in tetrahydrofuran (THF) and acetonitrile are displayed in Figure 2. These solvents were chosen because they represent the extremes of solvent polarity which were studied. The reaction free energy predicted by eq 4 (lines in Figure 2) is very sensitive to the radius parameters r_A and r_D in weakly polar solvents and insensitive to these parameters in strongly polar solvents. An "average" radius, r_X, of 4.5 Å was used in eq 4. This value is consistent with radii used by other workers in modeling similar molecules.

The FDPB model allows the "continuum solvent" to enter the cleft within **2**. It is not obvious how to model the dielectric response in this space because the steric constraints imposed by the donor, acceptor, and bridge restrict reorientation of the solvent molecules within the cleft. To probe the energetic consequences of the "cleft solvent", two kinds of FDPB calculations were performed for the $\Delta G°$ of **2**. In the first type, the dielectric constant of the cleft region was set equal to that of the bulk solvent (Figure 2, open symbols). In the second type, the bulk dielectric was excluded from the cleft by placement of a benzene ring in the cavity prior to determination of the solvent−solute boundary (Figure 2, filled symbols). This approach produces a dielectric constant of ∼2 within most of the cleft.

For **1** and **2** in acetonitrile, the results of the simple continuum model, eq 4, (Figure 2, solid lines) and the first FDPB model (open circles) are in excellent agreement. The predicted temperature dependence of $\Delta G°$ is very small. These results are not particularly surprising since minimal solvation correction is needed (acetonitrile is the reference solvent) and the Coulomb interactions between the ions is small for ϵ_{SOLV} ∼37. Exclusion of the dielectric from the cleft of **2** (filled circles) reduces $\Delta G°$ by ∼0.08 eV at all temperatures. This comparison demonstrates that eq 4 adequately describes the temperature dependence of $\Delta G°$ and its value at 295 K for **1** and **2** in acetonitrile.

For **1** and **2** in THF, $\Delta G°$ calculated with the above models are more divergent. The $\Delta G°(T)$ calculated by eq 4 is more exoergic and displays a slightly weaker temperature dependence than the prediction of the first FDPB model (open diamonds). Both differences result from use of large effective radii for the donor and acceptor in eq 4. If these radii are reduced to $r_A = r_D = 3.2$ Å for **1** and **2** in THF, the predicted $\Delta G°(T)$ values are in better agreement with the first FDPB model.[25] Exclusion of the dielectric from the cleft of **2** (filled diamonds) further reduces the predicted driving force by ∼0.1 eV.

The two FDPB models and eq 4 predict values of $\Delta G°$(295 K) that agree to within 0.3 eV. Given the potential impact an error in $\Delta G°$ might exert on the determination of $|V|$, $\Delta G°$(295 K) was treated as an adjustable parameter in the following analyses. Equation 4 and the FDPB analogues were used to calculate the *change* in driving force with temperature, $\Delta G°(T) - \Delta G°(295\ K)$. Best fit values of $|V|$ and λ_o(295 K) were obtained as a function of assumed values for $\Delta G°$(295 K) and λ_V. The range of $\Delta G°$(295 K) values used in the best fit determination of $|V|$ (see section IIIA) more than spans the range calculated with the above models. Also, since the FDPB models predict a different temperature dependence of $\Delta G°$ than does eq 4, both models were used in efforts to extract $|V|$ from the kinetic data.

C. Modeling the Solvent Reorganization Energy (λ_o). In these analyses of temperature-dependent k_{ET} data, the temperature dependence of λ_o is modeled and λ_o(295 K) is a fitting parameter. The temperature-dependent λ_o was written as

$$\lambda_o(T) = \lambda_o(295\ K) + \Delta\lambda_o(T) \tag{5}$$

As a consequence of the structure of eq 2, extracted values of the electronic coupling $|V|$ are sensitive to the modeling of the reorganization energy. This sensitivity was explored by consideration of the following three models for the reorganization energy.

In the first model, the temperature dependence of the index of refraction and the static dielectric constant were used to account for the temperature dependence of the low-frequency reorganization energy. The simplest approach calculated $\Delta\lambda_o(T)$ using the Marcus two sphere expression,[3a]

$$\Delta\lambda_o(T) = \frac{e^2}{2}\left(\frac{1}{r_A} + \frac{1}{r_D} - \frac{2}{R_{CC}}\right)\left[\left(\frac{1}{n(T)^2} - \frac{1}{\epsilon(T)}\right) - \left(\frac{1}{n(295\ K)^2} - \frac{1}{\epsilon(295\ K)}\right)\right] \tag{6}$$

$\Delta\lambda_o(T)$ was also calculated using the FDPB method.[12] The FDPB approach uses more realistic charge distributions and shapes for the DBA molecules than does the two sphere expression. The FDPB equation for λ_o is

$$\lambda_o = \frac{1}{2}\sum_i \Delta q_i(\phi_i^{\epsilon_o} - \phi_i^{\epsilon_\infty}) \tag{7}$$

where Δq_i is the change in charge at site i upon electron transfer

and ϕ is the electrostatic potential. More details of this model are provided elsewhere.[12,13,26]

The second model ignores the temperature dependence of λ_o and $\Delta G°$ by using the 295 K values of ϵ and n at all temperatures. This simplified approach was employed in prior analyses and is included here in order to connect with that work.[9]

The third model employs Matyushov's[14] molecular solvation theory to calculate $\lambda_o(T)$.[27] The low-frequency reorganization energy λ_o is written as the sum of two parts

$$\lambda_o = \lambda_p + \lambda_d \tag{8}$$

where λ_p accounts for the reorganization energy associated with solvent rotational degrees of freedom and λ_d accounts for the reorganization energy associated with solvent translational degrees of freedom. The rotational part λ_p has a temperature dependence that is determined by the Pekar factor, $(n(T)^{-2} - \epsilon(T)^{-1})$. The translational part λ_d has a temperature dependence that is given by

$$-\frac{1}{\lambda_d}\frac{\partial\lambda_d}{\partial T} = \frac{1}{T} + 2\alpha_T + \frac{4}{\epsilon_\infty(\epsilon_\infty + 2)}\frac{\partial\epsilon_\infty}{\partial T} \tag{9}$$

where α_T is the thermal expansivity of the solvent.

The temperature dependencies of λ_o that are predicted by these three models are qualitatively different. The first model predicts that λ_o decreases with temperature in weakly polar solvents and increases with temperature in strongly polar solvents. The Marcus and FDPB predictions of $\Delta\lambda_o(T)$ for **1** and **2** in acetonitrile agree to within 0.01 eV between 230 and 330 K (Figure 3). Not surprisingly, the best fit values of $|V|$ and λ_o(295 K) obtained using these models for $\Delta\lambda_o(T)$ agree to within ~10% (see section III). On the other hand, the magnitudes of λ_o(295 K) calculated using the Marcus and FDPB models differ by 0.26 eV for **1** and by as much as 0.48 eV for **2** (see Table 2). The two models treat the shape and charge distribution very differently, and this appears to influence the magnitude of λ_o but has little impact on $\Delta\lambda_o(T)$. The second model assumes that λ_o is temperature independent. The third model predicts that λ_o decreases with temperature both in weakly and strongly polar solvents. Although the rotational contribution, λ_p, increases slightly with increasing temperature, the translational contribution, λ_d, decreases more strongly.[14] The net decrease in λ_o from 230 to 330 K for **1** and **2** in acetonitrile (Figure 3) amounts to ~10% of λ_o(295 K). This prediction for $\Delta\lambda_o(T)$ generates significantly different, best fit values of $|V|$ and λ_o(295 K) compared to those obtained using models 1 and 2 (see section III).

Given the disparity between the predictions of the three models, the question arises whether any direct experimental data exist for comparison. Some spectroscopic evidence indicates that $\lambda_o(T)$ decreases with increasing temperature in weak to moderate polarity solvents.[28] The same cannot be said for the prediction, from model 1, that $\lambda_o(T)$ increases with increasing temperature in polar solvents. The intervalence absorption bands from symmetrical, localized, mixed valence compounds in aqueous solution are nearly temperature independent.[29] These studies indicate that $\lambda_o(T)$ is nearly temperature independent in aqueous solution. The temperature dependence of the charge-transfer absorption and emission bands of tetrahydro-4*H*-thiopyran-4-ylidenepropanedinitrile[30] were determined in a series of organic solvents.[31] The Stokes shift decreases with increasing temperature in solvents ranging in polarity from diethyl ether to acetonitrile. In charge-transfer theories, the Stokes shift is roughly equal to $2(\lambda_o + \lambda_V)$.[6,32] Because λ_V is solvent and temperature independent,[11b,29] the temperature dependence of the Stokes shift may be ascribed to λ_o. Thus, the Stokes shift from the thiopyran compound is in line with the predictions of model 3— not models 1 or 2. The best fit values of λ_o(295 K) and $|V|$ obtained using these three models for $\Delta\lambda_o(T)$ are discussed in the next section.

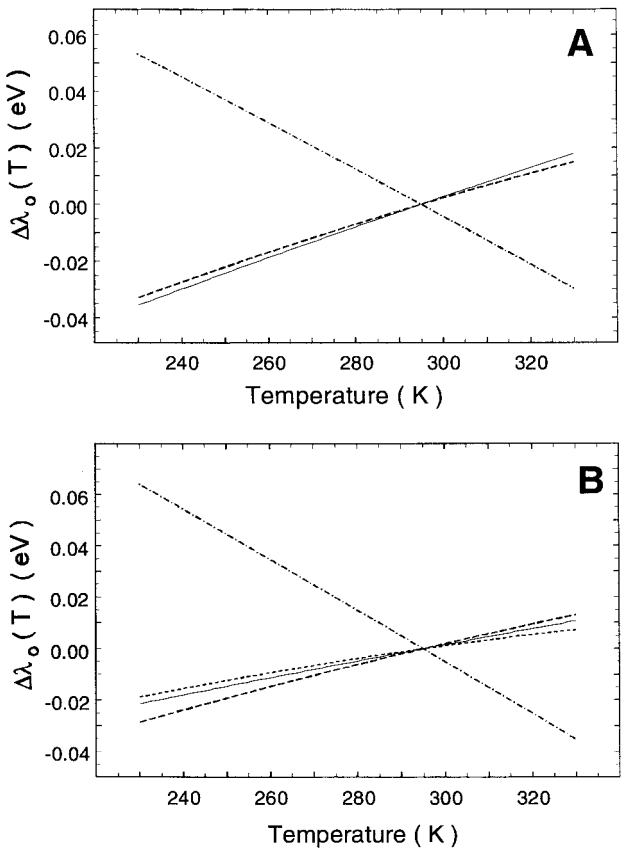

Figure 3. Comparison of eq 6 (solid line), FDPB model (dashed line), and Matyushov model (dashed dotted line) predictions of $\Delta\lambda_o(T)$ for **1** (panel A) and **2** (panel B) in acetonitrile. The short dashed curve in panel B is the FDPB model calculation for **2** with a benzene molecule placed in the cavity interior (see text).

III. One Mode Analysis of Electron Transfer for 1 and 2

The electron-transfer rate was measured as a function of temperature in each solvent. Figure 1 shows a plot of $\ln(k_{ET}T^{1/2})$ versus $1/T$ for **1** in acetonitrile. Similar plots were made for all of the systems discussed here. The rate constant data are supplied in the Supporting Information. Because the plot in Figure 1 is almost linear, it is only possible to extract two parameters, the intercept and the slope, whereas eq 2 has five parameters of which two are assumed to be temperature dependent. To proceed, the $k_{ET}(T)$ data was fit to eq 2 with $\Delta G°$(295 K), λ_V, and $\hbar\omega$ set to specific values. The temperature dependencies of $\Delta G°$ and λ_o were calculated using one of the models described in section II. In the remainder of this paper, method 1 refers to calculation of $\Delta G°(T) - \Delta G°$(295 K) using eq 4 and calculation of $\Delta\lambda_o(T)$ using eq 6, method 2 refers to use of temperature-independent values of $\Delta G°$ and λ_o, and method 3 refers to calculation of $\Delta G°(T) - \Delta G°$(295 K) using eq 4 and calculation of $\Delta\lambda_o(T)$ using Matyushov's model. For each method of simulating the temperature dependence of the FCWDS, the best fit to the kinetic data was obtained through variation of the two parameters $|V|$ and λ_o(295 K). The electronic coupling is most strongly correlated to the intercept

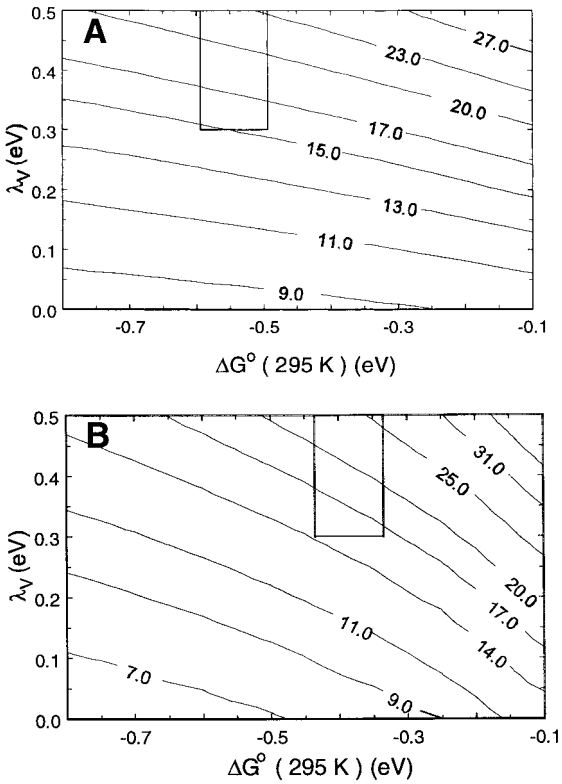

Figure 4. Contour plots of $|V|$ for **1** versus the assumed values of λ_V and $\Delta G°(295\ K)$, obtained from nonlinear regression analyses of the temperature-dependent k_{ET} data: (A) in acetonitrile, (B) in THF. The constant contour lines are in units of cm^{-1}. The box in each panel outlines the region defined by prior estimates of λ_V (0.3−0.5 eV) and $\Delta G°(295\ K) \pm 0.05$ eV predicted by eq 4. The temperature dependence of $\Delta G°$ was modeled with eq 4, and that of $\Delta\lambda_o(T)$ was calculated using eq 6.

and the solvent reorganization energy is most strongly correlated to the slope of Figure 1.

A. Analysis of 1. Figure 4 uses contour plots to illustrate the correlation between the $|V|$ parameter and two of the other parameters in eq 2, $\Delta G°(295\ K)$ and λ_V. In these figures, the temperature dependencies of the reorganization energy and of the Gibbs free energy were treated using the continuum model with temperature-dependent dielectric properties (method 1). Panels A and B in Figure 4 compare the two extreme cases of solvent polarity—acetonitrile and THF.

The contours of constant $|V|$ for **1** in acetonitrile (Figure 4A) are nearly parallel and almost straight lines. Horizontal contours would indicate that the extracted values of $|V|$ are independent of the value chosen for $\Delta G°(295\ K)$. The small slopes of the contours in Figure 4A indicate a weak dependence of the electronic coupling parameter on $\Delta G°(295\ K)$: about a 25% increase in $|V|$ is linked to a 0.6 eV increase in $\Delta G°$. In contrast, the best fit value (Figure 5) of the low-frequency reorganization energy $\lambda_o(295\ K)$ varies significantly with $\Delta G°(295\ K)$. These latter two parameters are strongly correlated, because they determine the apparent activation energy, i.e., the slope for the plot in Figure 1.[33] The best fit value of $|V|$ depends more strongly on λ_V than it does on $\Delta G°(295\ K)$ (Figure 4A), increasing by a factor of 2−3 as λ_V increases from 0 to 0.5 eV. Furthermore, the dependence on λ_V is relatively independent of $\Delta G°(295\ K)$. Similarly shaped contour plots are obtained upon analysis of the electron-transfer data for **1** in the polar solvents dimethylacetamide and benzonitrile (Supporting Information).

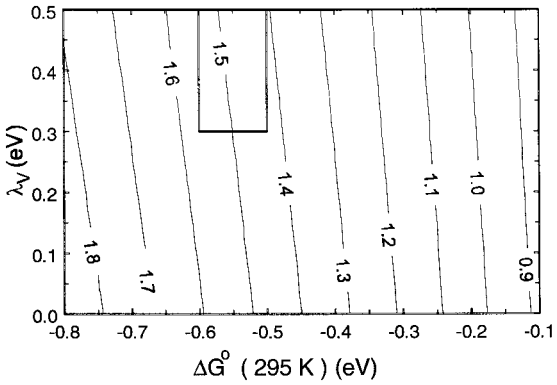

Figure 5. Contour plot of $\lambda_o(295\ K)$ for DBA **1** in acetonitrile versus the assumed values of λ_V and $\Delta G°(295\ K)$, obtained from nonlinear regression analysis of the temperature-dependent k_{ET} data. The constant contour lines are in units of eV. The box outlines the region defined by prior estimates of λ_V (0.3−0.5 eV) and $\Delta G°(295\ K) \pm 0.05$ eV predicted by eq 4. The temperature dependence of $\Delta G°$ was modeled with eq 4, and that of $\Delta\lambda_o(T)$ was calculated using eq 6.

Previously reported data for **1** in THF[9] were reexamined with this analysis, which accounts for the temperature dependence of $\Delta G°$ and λ_o (Figure 4B). The lines of constant $|V|$ in this plot are steeper, particularly at values of $\Delta G°(295\ K)$ approaching 0 eV. The significant temperature dependence of $\Delta G°$ for this system (see Figure 2B) produces a greater sensitivity of $|V|$ to the assumed value of $\Delta G°(295\ K)$. This result suggests that electronic couplings derived from temperature-dependent rate data in weakly polar solvents will be more sensitive to errors in $\Delta G°(295\ K)$ values than will couplings obtained from rate data in polar solvents.

The boxes in Figures 4 and 5 enclose regions corresponding to ± 0.05 eV about the $\Delta G°(295\ K)$ value calculated using eq 4 and λ_V in the range from 0.3 to 0.5 eV.[9b] These limits provide reasonable estimates of $|V|$ and $\lambda_o(295\ K)$. The mean values of $|V|$ determined for **1** within these constraints are similar (method 1 in Table 3) for all four of the solvents studied.[34] For **1**, the donor/acceptor electronic coupling does not appear to change significantly with solvent. This result indicates that either the electronic coupling is dominated by through bridge pathways, or the solvent mediated contributions are similar in each of these solvents (vide infra).

As a probe of the coupling magnitude's sensitivity to the modeling of the reorganization energy, the $k_{ET}(T)$ data from **1** was also analyzed using the other two $\Delta\lambda_o(T)$ models. $|V|$ listed under method 2 in Table 3 was obtained from contour plots in which the temperature dependencies of $\Delta G°$ and λ_o were ignored. The values obtained for the electronic coupling are about a factor of 3−4 smaller than those found by incorporating a temperature dependence for the dielectric constant and index of refraction (method 1, Table 3). $|V|$ listed under method 3 in Table 3 was obtained using $\Delta G°(T)$ from eq 4 and $\Delta\lambda_o(T)$ from the Matyushov model, which predicts a decrease in the reorganization energy with increasing temperature. This form for $\Delta\lambda_o(T)$ results in even smaller values of $|V|$. These comparisons show that the absolute magnitude of $|V|$ obtained from the data depends strongly on the modeling of $\Delta\lambda_o(T)$. Importantly, the relative values of $|V|$ in the various solvents are almost independent of which method is used to treat the temperature dependence of λ_o. In DBA **1**, $|V|$ is solvent independent.

The $\lambda_o(295\ K)$ values extracted from the data analyses were compared to the values of λ_o calculated using the simple Marcus and FDPB models. The range of reasonable $\lambda_o(295\ K)$ values

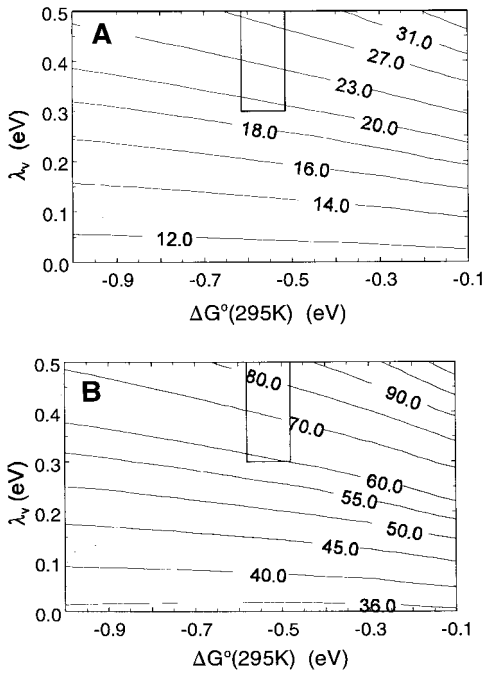

Figure 6. Contour plots of $|V|$ for **2** versus the assumed values of λ_V and $\Delta G°(295\ \text{K})$, obtained from nonlinear regression analyses of the temperature-dependent k_{ET} data: (A) in acetonitrile; (B) in benzonitrile. The constant contour lines are in units of cm^{-1}. The box in each panel outlines the region defined by prior estimates of λ_V (0.3−0.5 eV) and $\Delta G°(295\ \text{K}) \pm 0.05$ eV predicted by eq 4. The temperature dependence of $\Delta G°$ was modeled with eq 4, and that of $\Delta\lambda_o(T)$ was calculated with eq 6.

was determined from contour plots (e.g., Figure 5) in a manner analogous to the determination of reasonable $|V|$. The range of values for λ_o at 295 K is reported in Table 2. The parameters used in the Marcus expression were $r_D = r_A = 4.5$ Å and $R_{CC} = 11.5$ Å. For **1**, the estimates of $\lambda_o(295\ \text{K})$ from the method 1 data analysis are 0.40−0.46 eV larger than the Marcus values. If the effective radii r_A and r_D are reduced to 3.5 Å, λ_o calculated using the Marcus expression are within 0.1 eV of the method 1 results. The temperature-independent model for λ_o (method 2) produces smaller estimates of $\lambda_o(295\ \text{K})$ that are in line with the FDPB calculations. Use of $\Delta\lambda_o(T)$ based on the Matyushov model (method 3, Table 2) produces the smallest, experimentally derived values of $\lambda_o(295\ \text{K})$. These values happen to be in good agreement with the Marcus calculations based on 4.5 Å radii. Methods 1 and 3 use the same model for $\Delta G°(T)$. Hence, the 33% smaller estimates of $\lambda_o(295\ \text{K})$ from the latter are a direct consequence of the different treatments of $\Delta\lambda_o(T)$. The FDPB calculations of λ_o are larger than the Marcus results, are 0.2−0.3 eV smaller than the method 1 regression estimates and agree with the method 2 regression values. In conclusion, the simulation of $\Delta\lambda_o(T)$ with continuum models generates large values of $\lambda_o(295\ \text{K})$ from analyses of the kinetic data. Use of Matyushov's molecular model for $\Delta\lambda_o(T)$ produces significantly smaller values of $\lambda_o(295\ \text{K})$.

B. Analysis of 2. The analysis and parameter dependencies for **2** were similar to those found for **1**. The $|V|$ contour plots obtained for **2** are shown in Figure 6 and in the Supporting Information. The contour lines in Figure 6 are approximately parallel for large values of $-\Delta G°(295\ \text{K})$, and the spacing between the lines decreases as $-\Delta G°$ decreases. In sharp contrast to the results for **1**, the range of donor/acceptor coupling magnitudes for **2** vary significantly in different solvents: compare Figure 6A (acetonitrile) with Figure 6B (benzonitrile). In particular, the value of the electronic coupling for benzonitrile is anomalously large (Table 3). With the reasonable assumptions that λ_V is independent of solvent and $-\Delta G°$ in benzonitrile is less than or equal to $-\Delta G°$ in acetonitrile, the analysis shows that $|V|$ is four times larger in benzonitrile than in acetonitrile. The robustness of the large coupling in benzonitrile is underscored by a comparison of the couplings that were obtained using the three different methods of modeling $\Delta G°(T)$ and $\Delta\lambda_o(T)$. In each case, the coupling in benzonitrile is a factor of 3 to 5 times greater than for the other solvents (Table 3). Benzonitrile solvent mediates the donor/acceptor coupling in **2** more effectively than acetonitrile or dimethylacetamide.

Modeling of $\Delta\lambda_o(T)$ with the FDPB method caused small, but systematic, changes in the coupling magnitudes obtained for **2**. Two different FDPB calculations were implemented. In the first case, the dielectric surrounds the solute and is allowed to enter the cleft. This case yields electronic couplings of 22−33 cm^{-1} in acetonitrile, slightly higher than the values found using eq 6. In the second case, the dielectric is excluded from the clamp cavity and the FDPB model for $\Delta\lambda_o(T)$ yields electronic couplings of 17−26 cm^{-1}, slightly lower than those found using eq 6 (cf. method 1, Table 3). All three implementations of continuum models for $\Delta G°(T)$ and $\Delta\lambda_o(T)$ yield similar values of $|V|$, despite slightly different temperature dependencies.

The method 1 data analyses for **2** (Table 2) yield values of $\lambda_o(295\ \text{K})$ that are smaller than those found for **1** in the same solvent. This is expected as the donor/acceptor separation ($R_{CC} = 7.1$ Å) in **2** is smaller than in **1**. However, the observed reduction of $\lambda_o(295\ \text{K})$ from **1** to **2** is not as large as predicted by the Marcus or FDPB models. $\lambda_o(295\ \text{K})$ for **2** obtained using methods 2 and 3 (Table 2) are again smaller than from method 1 and in reasonable agreement with the FDPB calculations. The regression values of $\lambda_o(295\ \text{K})$ derived from methods 2 and 3 analyses increase slightly from **1** to **2** for the case of benzonitrile as solvent.[35] The $\lambda_o(295\ \text{K})$ values for dimethylacetamide and acetonitrile decrease as expected. All three analysis methods generate $\lambda_o(295\ \text{K})$ in benzonitrile that are distinctly larger than the Marcus and FDPB estimates. This may be related to the preeminent role of solvent mediated coupling for **2** in benzonitrile.

C. General Summary. The coupling magnitude for **2** in benzonitrile is substantially larger than the couplings determined for **1**, despite an additional two bonds[5b,30,36] and two s-cis links[30,36] in **2**'s bridge. In conjunction with the solvent independence of $|V|$ found for **1**, these results demonstrate that benzonitrile significantly enhances the donor/acceptor electronic coupling in **2**. The values of $|V|$ in dimethylacetamide and acetonitrile are also greater for **2** than for **1**, despite the longer, bent bridge in **2**.[30,36] These results suggest that the nonaromatic solvents may mediate donor/acceptor coupling in **2**, although to a smaller extent than benzonitrile. The χ^2 values from fits to the kinetic data using the three methods for $\Delta G°(T)$ and $\Delta\lambda_o(T)$ are similar and do not allow one to select from among the three models. Consequently, there is uncertainty in the magnitude of $|V|$ for a given DBA and solvent. The relative values of $|V|$ for a particular DBA in different solvents are much better defined. As the Matyushov model for $\Delta\lambda_o(T)$ is more in line with spectroscopic probes (vide supra), it seems that method 3 provides the best estimates of $\lambda_o(295\ \text{K})$ and $|V|$ (Tables 2 and 3).

IV. Two Mode and Classical Analyses for Electron Transfer in 1 and 2

The preceding analysis of the temperature-dependent electron-transfer data from **1** and **2** employed a single quantized mode,

semiclassical model for the electron-transfer rate constant. Raman studies of optical charge-transfer transitions[7] demonstrate that numerous modes can be active in such processes. This raises two questions relevant to this investigation: (1) How accurately does a single quantized mode model reproduce the temperature dependence of the FCWDS in a real DBA/solvent system, and (2) how sensitive are the extracted coupling magnitudes to the choice of the expression used to calculate the FCWDS? In an effort to establish additional confidence limits on the derived values of $|V|$, the data from **1** and **2** in acetonitrile and benzonitrile were analyzed using a classical model and a model with two quantized modes. These analyses modeled $\Delta G°(T)$ and $\Delta\lambda_o(T)$ using eqs 4 and 6, respectively.

The classical rate constant model assumes that only a classical degree of freedom is coupled to the reaction.[3a] The associated reorganization energy derives from both solvent and internal structural changes attending the reaction. The semiclassical model (eq 2) reduces to the classical model in the limit that $\lambda_V = 0$. For **1** and **2** in the solvents investigated, the "classical" $|V|$ ($\lambda_V = 0$ eV) is roughly half the semiclassical $|V|$ for $\lambda_V =$ 0.39 eV (see Figures 4 and 6). Importantly, the relative magnitudes of $|V|$, for different DBA molecules in the same solvent and the same DBA in different solvents, are nearly the same whether derived using the classical or the one quantized mode semiclassical model.

Two different forms of the two quantized mode, semiclassical model were used to analyze the electron-transfer rate data. In the first version, both modes were associated with high-frequency (>1000 cm^{-1}) vibrations. If the two modes have different frequencies, the one and two mode analyses return different values of $|V|$. While maintaining a constant total reorganization energy, $\lambda_V = \lambda_{V,1} + \lambda_{V,2}$, the effects of changing the second mode frequency and of partitioning the total λ_V between modes 1 and 2 were explored. The largest change in $|V|$, a reduction of 30% from the one mode to the two mode model, was obtained when the second mode corresponded to a very high-frequency vibration (e.g., 3000 cm^{-1} C−H stretch), and the majority of λ_V (0.29 eV out of 0.39 eV) was partitioned into this mode. The available Raman data[7] and C−H/C−D isotope effects on electron-transfer rate constants[37] do not indicate large reorganization energies associated with these high-frequency modes. Hence, it does not seem necessary to proceed beyond the two mode model. We conclude that inclusion of an additional high-frequency mode in the analysis, while maintaining a total λ_V that is consistent with the charge-transfer emission data,[9b] results in a slightly reduced (<30%) estimate of $|V|$.

In the second variant of the two mode model, the second mode was treated as intermediate in frequency[3b,28] (from 400 to 900 cm^{-1}). At the smaller vibrational frequencies, the model predicts an increase in the population of excited vibrational levels of the reactant state and an accompanying increase in the reaction rate with increasing temperature. This model produced smaller estimates of λ_o(295 K) and $|V|$ in the regression analyses. For example, when a λ_V of 0.4 eV is partitioned equally between a 1410 and a 400 cm^{-1} mode, a 2-fold decrease in $|V|$ and a 20−30% decrease in λ_o(295 K) is obtained from a best fit to the data, as compared to the one quantized mode results reported in Tables 2 and 3. Nevertheless, $|V|$ still shows a significant solvent dependence for **2**: 33 cm^{-1} in benzonitrile versus 13 cm^{-1} in acetonitrile. On the basis of this and other two mode analyses, it appears that changing the number of quantized modes produces, at most, a two- to 3-fold reduction in the estimates of $|V|$. However, the derived values of $|V|$ for every DBA/solvent combination are altered to a similar extent. Thus, the solvent *dependence* of $|V|$ in the clamp shaped molecule **2** and the solvent *independence* of $|V|$ in the linear molecule **1** are retained.

V. Analysis of Symmetry Allowed ET Reactions: Compounds 3 and 4

The data analyses for the "symmetry forbidden" molecules indicate that solvent mediated "pathways" contribute to the electronic coupling in the C-clamp **2** but are not detectable for **1**. It is interesting to investigate the magnitudes of bridge and solvent mediated coupling in molecules for which through bond electronic coupling is "symmetry allowed". Contour plots of $|V|$ as a function of $\Delta G°$(295 K) and λ_V were obtained for **3** and **4** in the same manner as for **1** and **2**. The values of $|V|$ are reported in Table 3, and the contour plots are in the Supporting Information. The modeling of these data incorporated the same characteristic frequency (0.175 eV) for the high-frequency mode and used an internal reorganization energy of 0.30 eV. Independent of the method employed to calculate $\Delta\lambda_o(T)$, $|V|$ in **3** and **4** are larger than in **1** and **2**. This observation is consistent with the earlier conclusion that the electronic symmetries of the initial and final states affect the magnitude of the electronic coupling.[9] The most direct measure of the symmetry effect is seen in a comparison of the couplings across the seven-bond, all trans bridge DBA molecules **1** and **3**. For the same solvent and method of calculating the FCWDS, $|V|$ in the symmetry allowed DBA **3** is 15−20 times larger than in the symmetry forbidden DBA **1**.[38]

Analysis of the kinetic data from **3** using continuum models for $\Delta\lambda_o(T)$ (method 1) generates estimates of $|V|$ larger than 200 cm^{-1}. Couplings of this magnitude indicate an electron-transfer reaction with adiabatic character. A self-consistent analysis of the rate data from **3** requires a formalism that interpolates between the nonadiabatic (eq 2) and adiabatic limits.[2b,39] As is true for **1** and **2**, the couplings obtained when the temperature dependencies of the dielectric parameters are ignored (method 2) are a factor of 3 to 4 smaller in magnitude. The couplings obtained using the Matyushov model (method 3) are another factor of 2−4 smaller. The values of $|V|$ obtained using either method 2 or 3 are consistent with the nonadiabatic rate constant model (eq 2). The couplings derived using method 3 are the same in acetonitrile and benzonitrile.[38] Although the $|V|$ obtained using method 1 and 2 also agree to within the quoted uncertainties in the two nitrile solvents, these limits refer to absolute uncertainties. More than 80% of the uncertainty in $|V|$ listed under methods 1 and 2 in Table 3 is associated with the variation of λ_V by ±0.1 eV. However, λ_V for the donor/acceptor pair in **3** is solvent (and bridge) independent. If a single λ_V value is chosen, e.g. 0.30 eV, the uncertainty in $|V|$ is reduced to less than 10 cm^{-1} for method 1 and less than 2 cm^{-1} for method 2. Taking into account only the uncertainty arising from $\Delta G°$, both methods 1 and 2 predict that $|V|$ is solvent dependent for **3**. This result is unexpected and indicates that these two methods do not adequately describe the FCWDS temperature dependence for **3**.

The λ_o(295 K) values obtained for **3** and **4** in the nitrile solvents exhibit reasonable trends. Independent of analysis method, λ_o(295 K) for **3** is ∼ 0.1 eV larger than for **1** in the same solvent. This is consistent with the longer charge-transfer distance in **3** (12.2 Å vs 11.5 Å for **1**). The reduction in λ_o(295 K) from acetonitrile to benzonitrile for **3** is in line with the Marcus and FDPB calculations. Only method 3 yields a notable decrease in λ_o(295 K) from **3** to **4**. This reduction is

about half that predicted by the continuum calculations. The large contribution of through solvent coupling for **2** in benzonitrile was accompanied by a larger λ_o(295 K) than for **1** in benzonitrile. This may be a signature of through solvent coupling and indicate some contribution of solvent mediation for **4** in acetonitrile. More definitive conclusions are not warranted on the basis of the λ_o results.

The three methods of treating the FCWDS temperature dependence do not produce consistent relative magnitudes of $|V|$ for **3** and **4** in acetonitrile. Methods 1 and 3 indicate $|V|$ is smaller for **4** than for **3**, whereas method 2 yields similar values of $|V|$. For **1**−**3**, Matyushov's treatment of $\Delta\lambda_o(T)$ gives the most self-consistent and reasonable coupling values and reorganization energy values. Choice of method 3 as the most valid simulation of the FCWDS temperature dependence leads to the conclusion that $|V|$ for **4** in acetonitrile is half as large as in **3.** The role of solvent mediated electronic coupling in **4** is not discernible from this result. An s-cis link within a covalent bridge is predicted to reduce through bond coupling matrix elements by a factor of between 2 and 30.[36] Thus, the elucidation of solvent's role must await determination of $|V|$ for **4** (and **3**) in benzonitrile and other polar solvents.

VI. Comparison of Experimental and Theoretical Values of $|V|$

The experimentally determined couplings in acetonitrile and benzonitrile are compared with couplings determined using ab initio methods in Table 4. The table also includes couplings previously derived[40] using the generalized Mulliken−Hush method.[41] For **2** and **4**, the latter calculations were performed either with no solvent or with a single nitrile molecule located at various positions between the donor and acceptor moieties. In the ab initio calculations, no attempt was made to perform statistical averaging as a function of solvent molecule orientations. The solvent molecule was placed in a geometry expected to enhance the electronic coupling.[42] For the symmetry allowed DBA molecule **4**, the solvent molecule was placed on the mirror plane symmetry element of the DBA and rotated such that it was in van der Waals contact with both the donor and the acceptor. For the symmetry forbidden DBA molecules **2**, the solvent molecule was displaced 1 Å away from the mirror plane symmetry element of the DBA and rotated to be in van der Waals contact with the donor and acceptor. The ab initio calculations of the electronic couplings were performed using the methods previously described.[43] The electronic coupling was calculated as half of the minimal energy splitting of the eigenstates composed mostly of the donor and acceptor sites as the energies of the latter are shifted into degeneracy.[44] The goal of these analyses was to probe any impact of the solvent molecule on the electronic coupling.

On a qualitative level, the theoretical calculations are in good accord with those extracted from the kinetic data using methods 2 and 3 for the FCWDS. The calculated in vacuo couplings for the linear molecules **1** and **3** are in reasonable accord with the experimental results (within a factor of 2). This confirms that solvent does not play a large role in promoting coupling in the linear DBA molecules. The two theoretical methods predict very different in vacuo couplings for the C-clamp molecule **4**. The ab initio method predicts that **4** incurs a small contribution from solvent mediated superexchange in acetonitrile as solvent. It is not feasible to compare the theoretical and experimental predictions for **4** as the latter has been determined in only one solvent.

The calculated couplings for the C-clamp molecule **2** agree with the experimental findings on a qualitative level. For the situation in which no solvent molecule is positioned between the donor and acceptor moieties of **2**, the calculated electronic couplings are quite small, <0.1 cm^{-1}. Introduction of a solvent molecule into the cleft produces a large increase in the calculated electronic coupling. Location of a solvent molecule outside of the cleft, but near either the donor or acceptor, has no significant influence on the electronic coupling.[40] The electronic coupling predicted by the two theories for a single benzonitrile molecule in the cleft agree with each other and are in reasonable accord with the experimental results. The two theories predict quite different couplings for the case of a single acetonitrile molecule in the cleft. The solvent mediated coupling magnitude is very sensitive to the position of the solvent molecules in the cleft.[40] The ab initio values reported here correspond to a single solvent geometry. A full theoretical treatment of this effect requires sampling of many configurations.[40] Despite some disparity in the absolute values of the couplings, the theoretical calculations confirm the role of solvent mediated coupling in the C-clamp shaped molecule **2** and the absence of solvent mediated coupling in the linear DBA molecules.

VII. Discussion

The success of semiclassical models in explaining the wide variety of electron-transfer kinetics and spectra has made it possible to use these models to probe the structural dependence of intramolecular, donor/acceptor electronic coupling matrix elements in a semiquantitative fashion. Nevertheless, extracting accurate values of $|V|$ from intramolecular electron-transfer rate constants is not trivial. All approaches to the problem require assumptions, which influence the magnitude of the extracted couplings. A general problem is the inability of experimentalists to obtain accurate values of $\Delta G°$ and λ_o. In the absence of forward−reverse electron-transfer equilibria, $\Delta G°$ must be obtained by some combination of redox potential measurements, solvation energy corrections, and Coulomb corrections. The availability of the FDPB[12] method, which incorporates details of molecular shape and charge distribution in calculations of neutral and ion solvation (and reorganization) energies, should help to mitigate this problem by providing a more refined method for computing $\Delta G°(T)$. Even with this method, care must be used when fitting temperature-dependent kinetics. Continuum models significantly underestimate the decrease in the driving force produced by increasing the temperature in polar solvents.[45] As a consequence, the temperature dependence of continuum calculations of $\Delta G°(T)$ and $\lambda_o(T)$ may be incorrect.

In polar solvents and for other conditions where Born solvation corrections are small, $\Delta G°$ calculated using the simple continuum model (eq 4) and the FDPB method are in good agreement. Under such conditions, the contribution of the Coulomb term to the energy tends to be small, so redox potentials and E_{00} dominate the $\Delta G°$ calculation. However, as donor/acceptor separations approach solvent molecule dimensions, steric impediments to solvent approach and restricted reorientation of solvent dipoles about the ions may reduce $\Delta G°$ relative to the predictions of eq 4. The FDPB method allows incorporation of some steric effects into the solvation calculations. For **2** in acetonitrile, FDPB estimates of this steric reduction in the driving force are ∼0.1 eV. In less polar solvents, Born solvation corrections become significant and appropriate estimates of the ion radii are needed for eq 4. Most donor and acceptor ions are not spherical, making determination of the most appropriate radii difficult. Using eq 4 with reasonable radii can easily produce $\Delta G°$ values that are in error (relative to FDPB calculations) by 0.1−0.2 eV. Taking into

account possible steric restrictions to solvation for small donor/acceptor separations, the simple continuum model can overestimate $-\Delta G°$ by 0.2−0.3 eV. The rate constant predicted by eq 2 is most sensitive to $\Delta G°$ when $-\Delta G° \ll \lambda_o$. Thus, incorrect values of $\Delta G°$ will produce the largest error in $|V|$ for reactions that are endoergic or nearly thermoneutral.

Clearly, the accuracy of simple continuum calculations of $\Delta G°$ is uncertain. Establishing confidence limits on $|V|$ obtained from rate constant data requires that the dependence on $\Delta G°$ be explored. Fortunately, when temperature-dependent rate constant data are analyzed, the uncertainty in $\Delta G°(295\ K)$ and small differences in $\Delta G°(T)$ produce small variation in the extracted coupling matrix element − at least for those cases where the reaction driving force does not approach 0 eV. In this investigation, variation of $\Delta G°(295\ K)$ over a 0.7 eV range produced less than a factor of 2 change in $|V|$. Use of slightly different forms for $\Delta G°(T)$ had nominal impact on $|V|$. By contrast, the value of $\lambda_o(295\ K)$ extracted from the data changed by an amount nearly equal in magnitude, but opposite in sign, to the variation in $\Delta G°(295\ K)$.

In contrast to the insensitivity of the extracted $|V|$ to the models used to calculate the temperature dependence of the $\Delta G°$, the model employed for the temperature dependence of λ_o strongly perturbs the derived value of the electron coupling. Simply ignoring any temperature dependence of λ_o (method 2) yields a slight solvent dependence of $|V|$ for the linear molecule **1** in four solvents and for the linear molecule **3** in highly polar solvents. Incorporation of a temperature dependence for λ_o (and $\Delta G°$) according to continuum models (method 1) produces 3- to 4-fold larger $|V|$ for **1** and **3**. While the $|V|$ for **1** obtained using method 1 is solvent independent, the $|V|$ obtained for **3** exhibits a rather substantial solvent dependence. Use of a molecular model for the temperature dependence of λ_o (method 3) yields solvent-independent $|V|$ for both **1** and **3** that are 2-fold smaller than those derived with method 2. $|V|$ for **1** and **3** are expected to be solvent independent. The bridge in both molecules is straight and lies between the redox centers, so that solvent inclusive electronic coupling pathways should contribute little to the overall coupling. Methods 2 and 3 generate the expected solvent independence of the coupling for **1** and **3**.[38] In addition, these two methods generate $|V|$ for **1** and **3** that bracket the matrix elements reported by Closs and Miller for coupling across the seven bond mostly-anti bridge in 2,6-disubstituted *trans*-decalins.[46] Although, the donor, acceptor, and attachment topology present in the decalins are different from those investigated here, it is reasonable that the symmetry allowed and symmetry forbidden topologies produce couplings that are larger and smaller, respectively, than those in the unsymmetrical decalins. These results argue for the use of methods 2 and 3, in preference to method 1, for simulation of the FCWDS temperature dependence. Overall, the results of this study demonstrate the large impact that the model for $\lambda_o(T)$ exerts on the derived values of $|V|$.

The combination of $|V|^2\ e^{-S}$ in the prefactor of eq 2 generates a strong correlation between S and $|V|$. Uncertainty in λ_V (or S) generates considerable uncertainty in $|V|$, as reflected by the contour plots presented in Figures 4 and 6. In general, increasing λ_V from 0 to 0.5 eV generates 2- to 3-fold increases in $|V|$. The number of quantized modes in the model has a similar effect on the magnitudes of $|V|$. Use of a two quantized mode model with a low-frequency mode produces a 3-fold smaller value for $|V|$.

Although the absolute magnitude of $|V|$ is strongly dependent on the choice of λ_V and the modeling of $\Delta\lambda_o(T)$, the relative magnitudes of $|V|$ for a particular donor/acceptor combination in different DBA molecules or different polar solvents are reasonably model independent. The insensitivity of the relative magnitudes of $|V|$ to the details of the modeling enables meaningful conclusions to be drawn regarding solvent and bridge effects on the electronic coupling. The present analysis demonstrates a strong solvent dependence of the electronic coupling magnitude for the C-clamp shaped molecule **2** but not for the linear molecules **1** and **3**.

The analysis of the kinetic data from **3** and **4** in THF does not produce useful information. The $|V|$ derived from the THF data differ by factors of 6−16 when methods 1 and 2 are used. This variation should be compared with the 3- to 4-fold variation in $|V|$ resulting from use of these two methods for **3** and **4** in acetonitrile and for **1** and **2**. The electron-transfer reactions for **3** and **4** in THF are close to thermoneutral. As a consequence, the regression results are very sensitive to the accuracy of the models used to simulate the temperature dependence of the FCWDS. For these molecules in THF, the accuracy of the regression results and the magnitude of the uncertainty limits are unacceptable. To address the question of through bond and through solvent coupling contributions for **4**, additional studies in polar solvents are required. Based on the results in acetonitrile, the coupling across the all-trans, seven-bond, symmetry allowed bridge in **3** is ∼15 times larger than across the all-trans, seven-bond, symmetry forbidden bridge in **1**. Also, if acetonitrile mediated coupling is active in **4**, it does not produce the same dramatic increase of the coupling as is evident for the symmetry forbidden C-clamp, **2**.

The three methods used to calculate the temperature dependence of the FCWDS yield values of $\lambda_o(295\ K)$ that vary by as much as 0.5 eV. Method 1 produces estimates of $\lambda_o(295\ K)$ that are the largest experimental values and which are much larger than the results of FDPB or two sphere Marcus calculations. Replacing the continuum model of $\Delta\lambda_o(T)$ with Matyushov's molecular model (method 3) yields estimates of $\lambda_o(295$ K) that are the smallest experimental values and which are in good agreement with the FDPB and Marcus calculations. Matyushov[14] has previously noted that his model and the Marcus model yield similar values of $\lambda_o(295\ K)$. Matyushov's model predicts a very different temperature dependence of λ_o than Marcus' model. In this investigation, the use of method 3 to calculate the temperature dependence of the FCWDS provides values of $|V|$ and $\lambda_o(295\ K)$ that are in good agreement with the best available theories and which are reasonably self-consistent.

Published experimental studies do not provide much guidance as to which values of $\lambda_o(295\ K)$ are most reasonable. For example, the λ_o reported for cyanoanthracene/alkylbenzene solvent separated ion pairs[5c] in acetonitrile (1.72 eV) are larger than the $\lambda_o(295\ K)$ found for **1** in acetonitrile (method 1), despite a smaller center to center separation in the ion pair. On the other hand, Miller and co-workers[47] found that the solvent contribution to the low-frequency reorganization energy is smaller than predicted by the Marcus model. The λ_o derived from the ion pair investigations[5c] may have significant contributions from ion motion in addition to solvent motion. Vibrational reorganization occurring in modes with low and intermediate frequencies have been documented.[47] Within the context of one mode rate constant models (eq 2), reorganization energy associated with such modes gets added to the low-frequency (solvent) reorganization term. Accordingly, extracted values of λ_o may be larger than continuum model predictions. The ester groups within the acceptors of **1** and **2** assume a more

planar conformation upon reduction.[9b] Breathing modes of the C-shaped bridge in **2** and **4** may be excited by electron transfer. These motions have low or intermediate frequencies and may contribute to the value of λ_o(295 K) extracted from the kinetic data. The magnitude of these contributions is not known.

This analysis of temperature-dependent rate data has explored the reliability of the values one obtains for electronic coupling matrix elements. It is clear that these coupling matrix element values are strongly dependent on the modeling of other parameters in the semiclassical equation (eq 2). The electronic coupling appears to be most strongly dependent on the value of λ_V and the temperature-dependent modeling of λ_o. The absolute value of the electronic coupling matrix element appears to be reliable to within a factor of 10. The estimates of λ_o(295 K) vary by about 0.3 eV depending on the model used for $\Delta\lambda_o(T)$. Importantly for the conclusions drawn from these data, the relative magnitude of the electronic couplings of similar systems (**1** to **2** and **3** to **4**) are less sensitive to the assumptions used to evaluate the FCWDS in eq 2. The relative magnitude of the couplings change by less than 50% with the various models. This reliability allows robust conclusions to be drawn concerning the importance of solvent mediated superexchange in **2**.

VIII. Conclusion

Electron-transfer rate constants for the DBA molecules were measured and analyzed using the semiclassical model for the rate constant. The goal of the analysis was to extract the electronic coupling magnitude. Because the semiclassical model has five parameters, the dependence of the electronic coupling parameter on the modeling of the other parameters in the rate expression was investigated. This study shows that although the absolute value of the electronic coupling $|V|$ cannot be determined with a certainty much better than an order of magnitude, the relative values of $|V|$ for the same DBA in different solvents or DBA molecules with the same D and A groups can be determined with greater confidence. For example, the values of the electronic coupling for **1** and **2** in acetonitrile and dimethylacetamide were of similar size, whereas their electronic coupling values in benzonitrile solvent were significantly different, independent of the model. This result supports the conclusion of previous work that the electronic coupling for **2** in benzonitrile solvent is enhanced. A comparison of the molecular structures for **1** and **2** in conjunction with theoretical calculation of the coupling supports the assignment of this enhancement to the solvent mediated superexchange. The development of accurate models for $\Delta\lambda_o(T)$ or direct measurements of $\Delta\lambda_o(T)$ would have a large impact on the ability to accurately determine $|V|$ from the temperature dependence of electron-transfer rate constants. Matyushov's molecular model for the solvent reorganization energy[14] appears to be the most appropriate model available for investigations in polar solvents.

Acknowledgment. This work was supported in part by the National Science Foundation (Grants CHE-9206765, CHE-9727657, CHE-9542939, and CHE-9416913). We are pleased to acknowledge informative discussions with Dr. D. Matyushov and the use of data collected by Drs. H. Han, Z. Lin, and Y. Zeng. We thank Dr. M. Newton (Brookhaven National Laboratory) and Professor R. Cave (Harvey Mudd College) for the GMH calculations for DBA **3** and **4**.

Appendix

The difference in the free energies of the CT state and the lowest energy, singlet excited state of the donor (LE), $\Delta G°$(LE→CT), may be obtained for any solvent (ϵ_{SOLV}) from the calculated solvation energies and the thermodynamic cycle displayed in the Chart 2. The first line in the cycle reflects the

Chart 2

$$DB_{ACN} + BA_{ACN} \rightarrow D^+B_{ACN} + BA^-_{ACN} \qquad E_{OX} - E_{RED}\ (2.49\ \text{eV in ACN})$$

$$D^+B_{ACN} + BA^-_{ACN} \rightarrow D^+B_{IN} + BA^-_{IN} \qquad -\Delta G^+_{SOLV(ACN)} - \Delta G^-_{SOLV(ACN)}$$

$$DBA_{IN} + D^+B_{IN} + BA^-_{IN} \rightarrow D^+BA^-_{IN} + DB_{IN} + BA_{IN} \qquad \Delta G^{IN}_{COULOMB}$$

$$D^+BA^-_{IN} \rightarrow D^+BA^-_{SOLV} \qquad \Delta G^{CT}_{SOLV}$$

$$DB_{IN} + BA_{IN} \rightarrow DB_{ACN} + BA_{ACN} \qquad \Delta G_{TRANS}$$

$$DBA_{SOLV} \rightarrow DBA_{IN} \qquad -\Delta G^{GS}_{TRANS}$$

$$D^*BA_{SOLV} \rightarrow DBA_{SOLV} \qquad -E_{00}$$

net: $D^*BA_{SOLV} \rightarrow D^+BA^-_{SOLV}$ $\quad \Delta G°(LE→CT)_{SOLV} = -E_{00} + E_{OX} - E_{RED} - \Delta G^+_{SOLV(ACN)} - \Delta G^-_{SOLV(ACN)} + \Delta G^{IN}_{COULOMB} + \Delta G^{CT}_{SOLV} + \Delta G_{TRANS} - \Delta G^{GS}_{TRANS}$

donor and acceptor redox potentials measured for the DB and BA molecules in acetonitrile (MeCN). The second line transfers the infinitely separated ions from acetonitrile to a medium with the same dielectric constant as that expected for the spacer, $\epsilon_{IN} \sim 2$. In this reference medium, transfer of both charges to the DBA is attended by an energy change calculated using Coulomb's law in a microscopically homogeneous dielectric medium. As this is a continuum approach, it does not correct for the finite size of solvent molecules (nonuniform continuum). However, this approach does employ Coulomb's law under conditions where it can be evaluated as a simple sum of interactions between partial charges. The fourth line transfers the CT state from a medium with dielectric constant ϵ_{IN} to one with the desired dielectric constant, ϵ_{SOLV}. The fifth line accounts for the solvation energy attending return of the neutral DB and BA models from a medium with dielectric constant ϵ_{IN} to acetonitrile. The sixth line accounts for the solvation energy required to move the neutral DBA molecule from a medium with the desired dielectric constant, ϵ_{SOLV}, to the medium with dielectric constant ϵ_{IN}. Incorporation of the experimentally determined S_1 (LE) state energy (seventh line) completes the thermodynamic cycle calculation of $\Delta G°$ (LE→CT) $_{SOLV}$.

Supporting Information Available: Tables listing electron transfer rate constant data for **1**−**4**, figures showing contour maps obtained using methods 1 and 3 for **1**−**4** and side and "cleft" views of DBA/solvent structures used to calculate $|V|$, and text describing the atomic radii calibration procedure used to calculate $\Delta G°$ and λ_o (25 pages). Ordering information is given on any current masthead page.

References and Notes

(1) Heitele, H. *Angew. Chem., Int. Ed. Engl.* **1993**, *32*, 359.
(2) (a) Onuchic, J. N.; Wolynes, P. G. *J. Phys. Chem.* **1988**, *92*, 6495. (b) Zusman, L. D. *Z. Phys. Chem.* **1994**, *186*, 1.

(3) (a) Marcus, R. A. *Annu. Rev. Phys. Chem*. **1964**, *15*, 155. (b) Jortner, J. *J. Chem. Phys*. **1976**, *64*, 4860.

(4) (a) Ulstrup, J.; Jortner, J. *J. Phys. Chem*. **1975**, *63*, 4358. (b)Yoshimori, A.; Kakitani, T.; Enomoto, Y.; Mataga, N. *J. Phys. Chem*. **1989**, *93*, 8316.

(5) (a) Rehm, D.; Weller, A. *Isr. J. Chem*. **1970**, *8*, 259. (b) Closs, G. L.; Miller, J. R. *Science* **1988**, *240*, 440. (c) Gould, I. R.; Young, R. H.; Moody, R. E.; Farid, S. *J. Phys. Chem*. **1991**, *95*, 2068. (d) Asahi, T.; Mataga, N.; Takahashi, Y.; Miyashi, T. *Chem. Phys. Lett*. **1990**, *171*, 309. (e) Pingyun, C.; Duesing, R.; Tapolsky, G.; Meyer, T. J. *J. Am. Chem. Soc*. **1989**, *111*, 8305. (f) DeGraziano, J. M.; Liddell, P. A.; Leggett, L.; Moore, A. L.; Moore, T. A.; Gust, D. *J. Phys. Chem*. **1994**, *98*, 1758.

(6) Marcus, R. A. *J. Phys. Chem*. **1989**, *93*, 3078.

(7) (a) Myers, A. B. *Chem. Rev*. **1996**, *96*, 911. (b) Kulinowski, K.; Gould, I. R.; Myers, A. B. *J. Phys. Chem.* **1995**, *99*, 9017. (c) Doorn, S. K.; Hupp, J. T. *J. Am. Chem. Soc*. **1990**, *112*, 1142, 4999. (d) Wynne, K.; Galli, C.; Hochstrasser, R. M. *J. Chem. Phys*. **1994**, *100*, 4797.

(8) (a) Finckh, P.; Heitele, H.; Volk, M.; Michel-Beyerle, M. E. *J. Phys. Chem*. **1988**, *92*, 6584. (b) Closs, G. L.; Miller, J. R.; Liang, N. *J. Am. Chem. Soc*. **1989**, *111*, 8740. (c) Harriman, A.; Heitz, V.; Sauvage, J.-P. *J. Phys. Chem*. **1993**, *97*, 5940.

(9) (a) Zeng, Y.; Zimmt, M. B. *J. Am. Chem. Soc.* **1991**, *113*, 5107. (b) Zeng, Y.; Zimmt, M. B. *J. Phys. Chem*. **1992**, *96*, 8395.

(10) Kumar, K.; Lin, Z.; Waldeck, D. H.; Zimmt, M. B. *J. Am. Chem. Soc*. **1996**, *118*, 243.

(11) (a) Heitele, H.; Finckh, P.; Weeren, S.; Pöllinger, F.; Michel-Beyerle, M. E. *J. Phys. Chem*. **1989**, *93*, 5173. (b) Hupp, J. T.; Neyhart, G. A.; Meyer, T. J.; Kober, E. M. *J. Phys. Chem.* **1992**, *96*, 10820. (c) Kroon, J.; Oevering, H.; Verhoeven, J. W.; Warman, J. M.; Oliver, A. M.; Paddon-Row: M. N. *J. Phys. Chem*. **1993**, *97*, 5065.

(12) (a) Sharp, K.; Honig, B. *Annu. Rev. Biophys. Biophys. Chem*. **1990**, *19*, 301. (b) Sitkoff, D.; Sharp. K. A.; Honig, B. *J. Phys. Chem*. **1994**, *98*, 1978.

(13) (a) Kurnikov, I. V.; Zusman, L. D.; Kurnikova, M. G.; Farid, R. S.; Beratan, D. N. *J. Am. Chem. Soc*. **1997**, 5690. (b) Liu, Y. P.; Newton, M. D. *J. Phys. Chem*. **1995**, *99*, 12382.

(14) (a) Matyushov, D. V. *Chem. Phys*. **1993**, *174*, 199. (b) Matyushov, D. V. *Mol. Phys*. **1993**, *79*, 795.

(15) Gould, I. R.; Noukakis, D.; Goodman, J. L.; Young, R. H.; Farid, S. *J. Am. Chem. Soc*. **1993**, *115*, 3830.

(16) The 3 and 4 bond analogues are structures **8**−**9** in ref 9b.

(17) Table 4 of ref 9b lists two (λ_V, ω) pairs for each D/A pair. Since publication of that work, two additional (λ_V, ω) pairs have been found which generate excellent fits of the CT emission spectra.

(18) Kulinowski, K.; Gould, I. R.; Myers, A. B. *J. Phys. Chem.* **1995**, *99*, 9017.

(19) Although most of our description proceeds in terms of λ_V and ω, a better choice for exploring the impact of individual parameters on $|V|$ are S and ω. In this partitioning, the latter term only appears in the classical activation energy portion of eq 2, and the former appears in the nuclear tunneling factor.

(20) The range of λ_V used varies S substantially more than would variation of ω by 200 cm^{-1}.

(21) Rehm, D.; Weller, A. *Z. Phys. Chem.* (*Munich*) **1970**, *69*, 183.

(22) Tachiya, M. *Chem. Phys. Lett*. **1994**, *230*, 491.

(23) Zhang, L. Y.; Friesner, R. A. *J. Phys. Chem.* **1995**, *99*, 16479.

(24) (a) Besler, B. H.; Merz, K. M., Jr.; Kollman, P. A. *J. Comput. Phys.* **1990**, *11*, 431. (b) Singh, U. C.; Kollman, P. A. *J. Comput. Phys.* **1984**, *5*, 12.

(25) Use of $r_A = r_D = 3.2$ Å for **1** and **2** in acetonitrile does not significantly alter the predicted temperature dependence or magnitude of ΔG.

(26) The calculated reorganization energies for a charged molecule are roughly inversely proportional to the solute atomic radii. The radius parameters used in the FDPB method were determined in the manner described for the computation of $\Delta G°$.

(27) Inclusion of Matyushov's formulation of temperature dependent, translational contributions to $\Delta G°$ resulted in regression estimates of $|V|$ and λ_o(295 K) that were physically unreasonable. Thus, the temperature dependent, translational contribution for only λ_o was modeled.

(28) Cortés, J.; Heitele, H.; Jortner, J. *J. Phys. Chem.* **1994**, *98*, 2527.

(29) Dong, Y.; Hupp, J. T. *Inorg. Chem.* **1992**, *31*, 3322.

(30) Pasman, P.; Rob, F.; Verhoeven, J. W. *J. Am. Chem. Soc*. **1982**, *104*, 5127.

(31) Vath, P.; Zimmt, M. B. To be submitted for publication.

(32) Gould, I. R.; Noukakis, D.; Gomez-Jahn, L.; Young, R. H.; Goodman, J. L.; Farid, S. *Chem. Phys.* **1993**, *176*, 439.

(33) The systems studied here are weakly exoergonic. Hence, the first term in the sum of eq 2 dominates the contribution to the rate constant. In this case $\Delta G°$ and λ_o determine the slope.

(34) The error bounds reported for the couplings were obtained by determining the range of $|V|$ values in the boxed region of the contour plot.

(35) λ_o(295 K) obtained with method 1 for **1** and **2** in benzonitrile are almost identical.

(36) (a) Oliver, A. M.; Craig, D. C.; Paddon-Row, M. N.; Verhoeven, J. W. *Chem. Phys. Lett.* **1988**, *150*, 366. (b) Oevering, H.; et. al. *J. Am. Chem. Soc.* **1987**, *109*, 3258. (c) Hoffman, R. *Acc. Chem. Res.*, **1971**, *4*, 1. (d) Gleiter, R. *Angew. Chem., Int. Ed. Engl*. **1974**, *13*, 696. (e) Paddon-Row, M. N.; Patney, H. K.; Brown, R. S.; Houk, K. N. *J. Am. Chem. Soc.* **1981**, *103*, 3, 5575. (f) Liang, C.; Newton, M. D. *J. Phys. Chem.* **1992**, *96*, 2855.

(37) Gould, I. R.; Ege, D.; Moser, J. E.; Farid, S. *J. Am. Chem. Soc.* **1990**, *112*, 4290.

(38) The electron-transfer reaction of **3** in THF is too close to thermoneutral to provide useful estimates of $|V|$. (See the discussion in section VII.)

(39) (a)Beratan, D. N.; Onuchic, J. N. *J. Chem. Phys*. **1988**, *89*, 6195. (b) Calef, D. F.; Wolynes, P. G. *J. Phys. Chem.* **1983**, *87*, 3387. (c) Rips, I.; Jortner, J. *J. Chem. Phys*. **1987**, *87*, 2090. (d) Garg, A.; Onuchic, J. N.; Ambegaokar, V. *J. Chem. Phys*. **1985**, *83*, 4491. (e) Use of such rate constant models was explored, but the resulting $|V|$ were only 20−30% smaller than those reported under method 1 in Table 3.

(40) Cave, R. J.; Newton, M. D.; Kumar, K.; Zimmt, M. B. *J. Phys. Chem.* **1995**, *99*, 17501.

(41) Cave, R. J.; Newton, M. D. *Chem. Phys. Lett*. **1996**, *249*, 15.

(42) See the Supporting Information for views of the DBA/solvent complexes studied with ab initio methods.

(43) (a) Kurnikov, I. V.; Beratan, D. N. *J. Chem. Phys.* **1996**, *105*, 9561. (b) Kurnikov, I. V.; Zusman, L. D.; Kurnikova, M. G.; Farid, R. S.; Beratan, D. N. *J. Am. Chem. Soc*. **1997**, *119*, 5690.

(44) The effective electronic Hamiltonian of the system was derived from separate Hartree−Fock calculations on fragments of the system involving donor, acceptor, and bridging groups[43a] and from Hartree−Fock calculation on the entire systems. The coupling values obtained with and without use of the fragmentation technique differed by less than 20%. The donor and acceptor states appeared as unoccupied orbitals of the effective electronic Hamiltonian. IVO corrections[43b] were introduced to improve the virtual orbital description of excited donor states. The 3-21G and 6-311G basis sets were used in the Hartree−Fock calculations. CIS (configuration interaction singles) on the molecules were also employed to obtain the electronic coupling data. In this case, the coupling was calculated from the energy splitting of the two lowest CIS eigenstates that corresponded to donor and acceptor states. The donor and acceptor energies were shifted into resonance by attaching point charges to the donor and acceptor groups. The 3-21G basis set was used for CIS calculations. The CIS results agreed to within 30% with those derived using the Hartree−Fock/effective Hamiltonian method.

(45) (a) Jaworski, J. S. *J. Electroanal. Chem.* **1987**, *219*, 209. (b) Svaan, M.; Parker, V. D. *Acta Chem. Scand., Ser. B* **1984**, *38*, 751.

(46) Closs, G. L.; Miller, J. R. *Science* **1988**, *240*, 440.

(47) (a) Miller, J. R.; Paulson, B. P.; Bal, R.; Closs, G. L. *J. Phys. Chem.* **1995**, *99*, 6923. (b) Newton, M. D.; Basilevsky, M. V.; Rostov, I. V. *Chem. Phys.*, submitted for publication.